

EFFECTS OF HYDROGEN INDUCTION IN A DIESEL ENGINE OPERATING WITH BIODIESEL B20 AT DIFFERENT INJECTION TIMINGS

Iulian VOICU, Radu CHIRIAC, Nicolae APOSTOLESCU

„POLITEHNICA“ UNIVERSITY – BUCHAREST

Abstract. The blended biodiesel with up to 20% biodiesel in petroleum diesel (B20) is considered as available in production. Previous studies investigating the effect of B20 on engine emissions led to some contradictory results. The present study continued the investigation on B20 effects and was also extended on B20 enriched with hydrogen. It was conducted on a conventional tractor diesel engine running alternatively with B20 and petroleum diesel at various speeds and full load and then, with the same fuels enriched with hydrogen, at 60% load and two speeds. It was found that compared with petroleum diesel, the engine fueled with B20 has higher NO_x emissions at all speeds and lower smoke and CO emissions while both fuels combustion closely resembles. The possibilities to enhance the effects of hydrogen addition to B20 fuel by modifying the injection timings were also explored by numerical simulation of the engine operation using the AVL BOOST v2011.1 code.

1. INTRODUCTION

Biodiesel is considered an attractive fuel, which is renewable and offers, from a life-cycle perspective, an important decreased atmospheric carbon emission compared with conventional diesel fuels. Its reported advantages include generally lower emissions of CO, hydrocarbons HC and particulate matter PM, but with eventually increased NO_x emissions compared to fossil diesel fuels. The influence on the engine efficiency is typically slight [1...9]. The properties comparison with diesel fuel includes lower heating value, higher bulk modules of compressibility and viscosity, less favorable cold flow properties. European car manufacturers approved 5% of biodiesel blend in fossil diesel fuel (B5 fuel), which meets European fuel standards EN 14214 and EN 590. The current ASTM D975-09B specification for petroleum diesel fuel in United States allows also up to 5% (by volume) biodiesel [10].

Biodiesel consists of alkyl-monoesters of fatty acids (generally methyl-esters), which are converted from vegetable oil or animal fats by a process of transesterification. The most common vegetable feedstock is rapeseed oil in Europe and soybean oil in United States; other vegetable sources like peanut oil or cottonseed oil and animal fats like used cooking grease and beef tallow are also used for biodiesel production [11]. These basic oils and fats have fatty acids of different compositions and various proportions resulting in a corresponding variety of methyl esters that compose biodiesel.

The rapeseed oil and soybean oil are composed, for example, of 5 common fatty acids, in widely varying proportions; one more fatty acid compose only the rapeseed oil, but with 50.9% mass [12]. The differences in chemical composition are eventually reflected in fuel properties and ultimately influence the combustion process, controlling the engine performance, efficiency and emission formation. The blends of biodiesel with petroleum diesel fuel have intermediate properties, but their relative differences are not proportional with the percentage amount of biodiesel.

The complex influence of these differences in fuel properties on the process in the engine cylinder, as well as the different experimented engines and the various test conditions, can explain some apparently contradictory or inconsistent results reported in the literature.

Extensive studies [13, 14] have shown the possibility to operate compression ignition engines on biodiesel with very little or no engine modifications due to the similar properties of biodiesel to mineral diesel fuel. Some increasing in fuel consumption in approximate proportion to the loss of heating value was reported. Concerning emissions, the use of biodiesel in conventional diesel engines resulted in substantial reduction of unburned hydrocarbons, carbon monoxide and a high consensus was found in the sharp reduction in particulate emissions.

Other study [15] conducted on a Caterpillar diesel engine of 74.6 kW at 2100 rpm, running at high load, reported differences between some blends

of biodiesel (soybean methyl esters) in fossil fuel. With a single injection and start of injection of 7 CA BTDC at full load, a 20% biodiesel blend (B20) leads to 6.5% higher CO and PM emissions, than the neat fossil fuel, while with 40% biodiesel (B40), CO and PM emissions were 13% and 26% correspondingly lower than with neat diesel fuel. The CO and PM emissions were but lower by 5% and 4% correspondingly with B20 by changing the start of injection to 4 CA BTDC and with B40 lower by 20% and 35% correspondingly. At low load, a similar trend was found for both biodiesel blends, B20 and B40, with PM emissions higher and CO emission lower than for diesel fuel.

The potentialities of hydrogen as a complementary fuel, for biodiesel, previously explored with petroleum diesel fuel in terms of engine performance, efficiency and emissions were also explored in the last years. NO_x emission was not influenced with the hydrogen input, but the NO₂/NO_x proportion was raised by hydrogen addition. The most notable changes occurred with less than 10% hydrogen (by energy) input [16...18].

A study on the effects of hydrogen addition to neat biodiesel was initiated recently by Bika et al. [19]. A passenger car engine of 66 kW at 3750 rpm was fueled with biodiesel B99 (soybean methyl ester) and additional hydrogen was injected into the intake manifold. The investigation was carried out at 1700 rpm and various loads. Lower PM (mass fraction) by 12% with 5% hydrogen input (by energy) and by 22% with 20% hydrogen were reported at mid load, but no significant results were found at high load.

In the present work, performance and emissions of a tractor diesel engine operated in dual-fuel mode were experimentally investigated. The effects of hydrogen addition to a 20% (by volume) biodiesel blend (B20) as main fuel were compared with the condition of hydrogen supplementing commercial petroleum diesel fuel. In the second part of this work, possibilities to enhance the effects of hydrogen addition to B20 fuel by modifying the injection timing were also explored by numerical simulation of the engine operation with the AVL BOOST v2011.1 code.

The 20% biodiesel blend was prepared with neat biodiesel (B100) rapeseed methyl ester, RME and commercial diesel fuel Euro 5 (B0). Table 1 shows some properties of diesel fuel and biodiesel.

2. EXPERIMENTAL SET-UP AND TEST PROCEDURE

The test engine was a naturally aspirated direct injection tractor diesel engine with 4 cylinders in line having the total capacity of 3759 cm³, nominal power of 50 kW at 2400 rpm, maximum torque of 228 Nm at 1400 rpm, and the compression ratio of 17.5. The engine injection system was Delphi comprising a DP210 rotary pump and injectors with 5 holes of 0.24 mm diameter. The schematic of the experimental set up is shown in Figure 1, with the symbols of the main components. The test bed was correspondingly equipped in order to collect and acquire the relevant parameters characterizing the engine operation condition. Technical hydrogen (purity 99.98%) supplied by SIAD and stored in special bottles at high pressure was introduced through a dedicated line at low pressure to the engine intake manifold.

This line was provided with pressure regulators, two pressure gauges, two thermocouples, an electronic precision gas flow meter type ALICAT Scientific M series, two flame arrestors equipped with one way valve and an emergency rapid stop valve. The instrumentation was adequately selected to ensure safety operation and monitoring of the engine when it was partially fueled with the potentially explosive hydrogen gas. Concerning the engine operating parameters, the instant torque and speed were measured and controlled by an eddy current dynamometer type AVL Alpha 160. Engine air consumption was measured by means of a volumetric flowmeter type SCHLUMBERGER Fluxi 2000/TZ. The fuel consumption was measured with an AVL Dynamic Fuel Meter 733 S provided with an AVL Fuel Temperature Controller 753 C. The exhaust emissions (CO₂, CO, NO_x and THC) were measured by an exhaust gas analyzer (HORIBA Mexa 7170 D) which calculates and provides the relative air-fuel ratio value too. The smoke level in the exhaust gases was measured with an AVL Smoke Meter 415 S. All the global engine operating parameters including temperatures and pressures of cooling water, oil, air, exhaust gases and test cell atmosphere were measured with adequate devices and registered by the AVL Puma Open v1.4 equipment. Pressure traces have been recorded for two engine cylinders (1 and 3) with an AVL data acquisition system composed from: quartz pressure transducers AVL GM 12 D,

Table 1

Fuel properties

Property	Diesel, B0	RME, B100
Density @ STP, kg/m ³	820	882
LHV, MJ/kg	42.8	≈ 37
Cetane number	51	54
Viscosity at 40°C, cSt	2	4.2

AVL 3066A02 charge amplifiers, and crank angle encoder AVL 365 C. The cylinder number 1 was also provided with a Perkins-Lucas injector supplied by WOLFF Controls Corporation (WCC) and equipped with a Hall Effect Position Sensor for the needle lift recording. For the same injector, its high pressure pipe was outfitted with an AVL QL21D high pressure transducer (3000 bar) and an AVL 3066A01 charge amplifier. Pressure at the injection pump was measured with an AVL 31 DP pressure transducer connected to an AVL 3009 A03 charge amplifier. The injection pressure was thus simultaneously recorded at the pump and injector level. Finally all these instruments have been connected to the data acquisition module AVL Indiset 620 provided with the AVL Indicom 1.6 software for data collection and manipulation. For each opera-

ting point during the test program 200 consecutive cycles and an average cycle over them were registered. During experiments the oil temperature was controlled in the range $90 \pm 1^\circ\text{C}$ by means of a dedicated oil heat exchanger provided with electro valves for oil and cooling water and with two temperature controllers type OMRON E5CN. Water temperature was in the range $70\text{-}75^\circ\text{C}$.

Test conditions selected were at part load operation (60%) and two speeds, 1400 rpm (maximum torque speed) and 2400 rpm (maximum power speed). The different additions of hydrogen were accompanied each time by a corresponding decrease of the main fuel (commercial diesel fuel or B20) flow, to keep constant the engine operating condition (dynamometer on constant torque-speed operation mode).

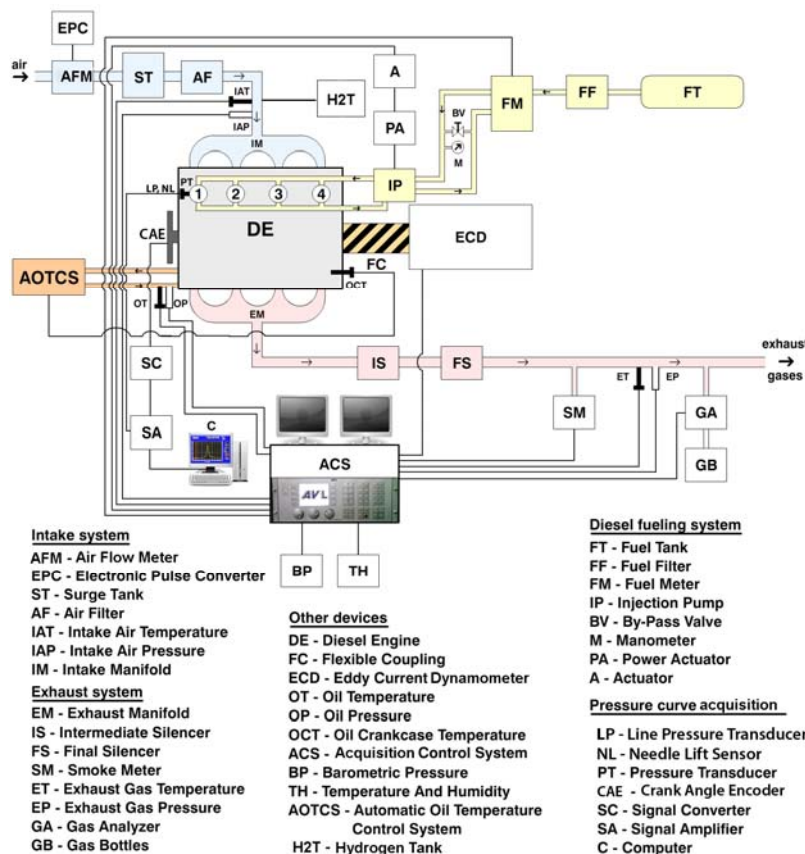


Fig. 1. Schematic layout of the test bench.

3. EXPERIMENTAL RESULTS

3.1. Efficiency and combustion characteristics

Addition of hydrogen has no significant influence on brake thermal efficiency (BTE). At 1400 rpm, BTE with B20 is lower by about 1% in comparison with diesel fuel, and the effect of hydrogen is negligible (Figure 2a). At 2400 rpm, BTE with B20 is higher by 2% than with diesel

fuel, with a similar lack of the hydrogen addition influence (Figure 2b).

The effect of hydrogen supplement on the averaged cylinder pressure traces and the corresponding combustion characteristics (Figures 3, 4) were minimal. Pressure traces and the rate of heat release characteristics show that there is apparently no difference between diesel and B20 fuel while the hydrogen presence slightly modifies the position of the rate of heat release.

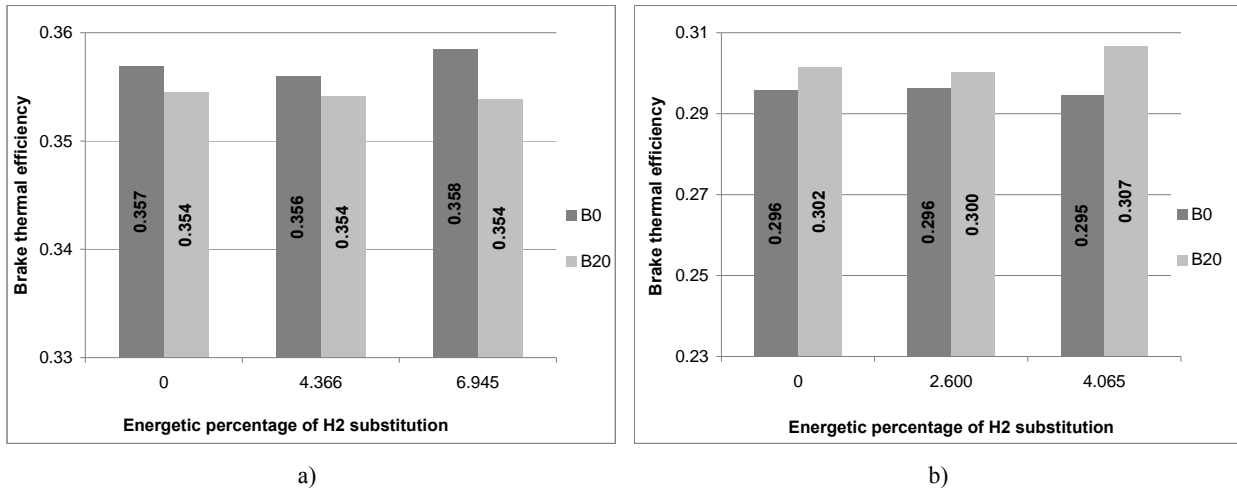


Fig. 2. Variation of BTE with hydrogen fraction (energy) at 60% load:
 a – 1400 rpm; b – 2400 rpm, for diesel fuel and B20.

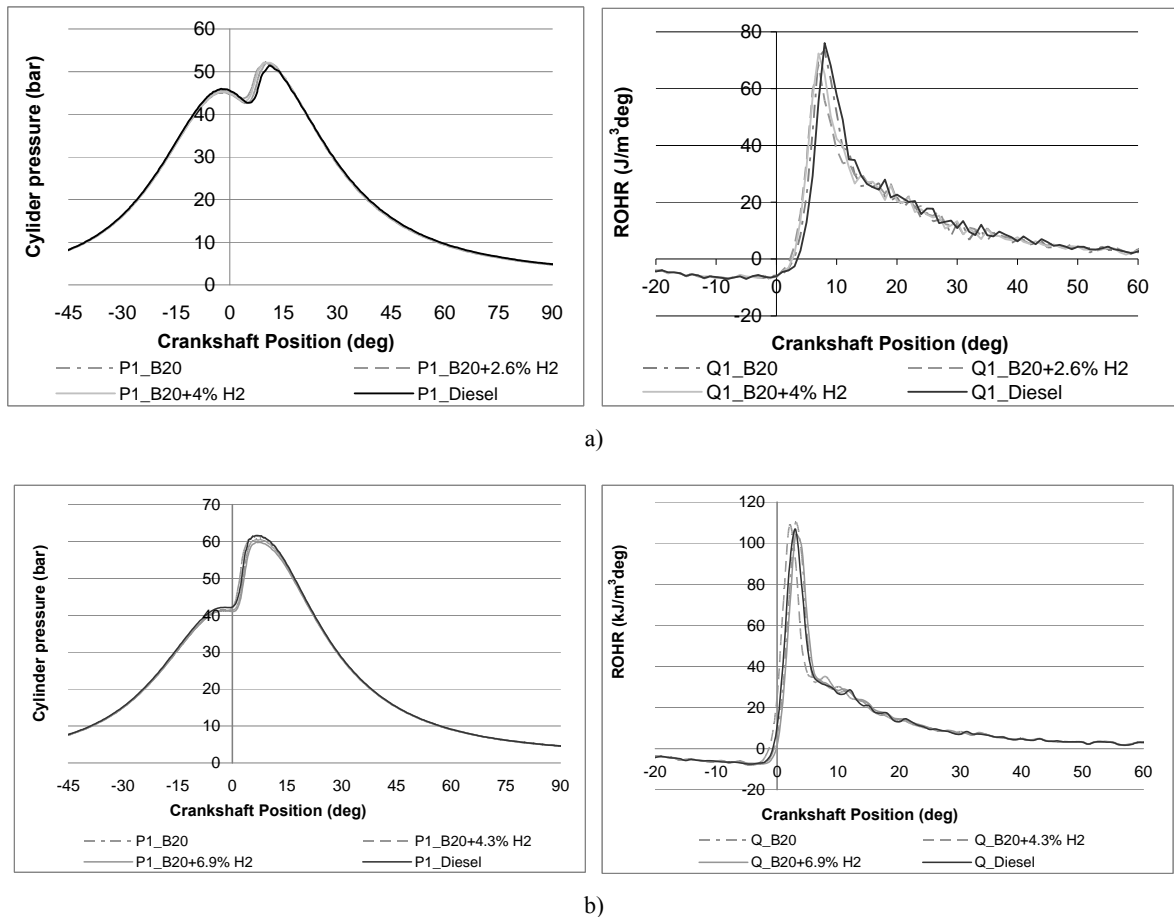


Fig. 3. Variation of pressure and rate of heat release for B20 and diesel fuel B0 with hydrogen percentage at 60% load:
 a – 1400 rpm; b – 2400 rpm.

Figure 4 shows the characteristic moments of the heat release at 60% load and 2400 rpm. The start of combustion α_i accepted as the moment when the rate of heat release becomes positive, shows differences less than 0.5°CA for the base fuels (petroleum diesel fuel B0 and B20).

The start of injection is advanced by about 0.25°CA for B20, which is attributed to the higher density, bulk modulus of compressibility and speed of sound relative to the petroleum diesel fuel. This effect, associated with a small reduction on ignition delay would result in the slight advance of the

moment α_i for B20. An effect of hydrogen addition on the autoignition stage, thus on the moment α_i is almost imperceptible. The hydrogen aspirated in the intake air results in a homogeneous mixture before the liquid fuel injection, with a concentration well below the lean limit of flammability. Moreover a possible active role of hydrogen in the hydrocarbon autoignition mechanism in the diesel engine cylinder is not known. The presence of hydrogen is likely to increase the heat release rate in the premixed combustion phase, with the temperature at the beginning of the mixing controlled phase correspondingly slightly higher. Durations almost equal for the initial phase of combustion ($\Delta\alpha$ 10%) and the first part of the mixing controlled combustion phase ($\Delta\alpha$ 50%) are apparent for both main fuels and various proportions of hydrogen.

A significant effect of hydrogen addition is but apparent on the durations of 90% heat release ($\Delta\alpha$ 90%) for base fuels with apparently no significant consequence on BTE. At 2400 rpm the interval between α 90% and α 50% — which would correspond to the heat release interval in the second part of the mixing-controlled combustion phase — is longer for base fuels with 6.5°CA or 23%, and 5.8°CA or 20.5%, by addition of 2.6% and 4% hydrogen, respectively. The same interval is longer by addition of 4.4% hydrogen with 5.5°CA or by 17% at 1400 rpm. Since the rate of heat release is controlled in this phase by the rate of fuel-air mixing process, the results would suggest a generally worse condition of mixing with hydrogen enrichment of the aspirated air. A similar effect of hydrogen addition was found for diesel fuel in a previous work [18].

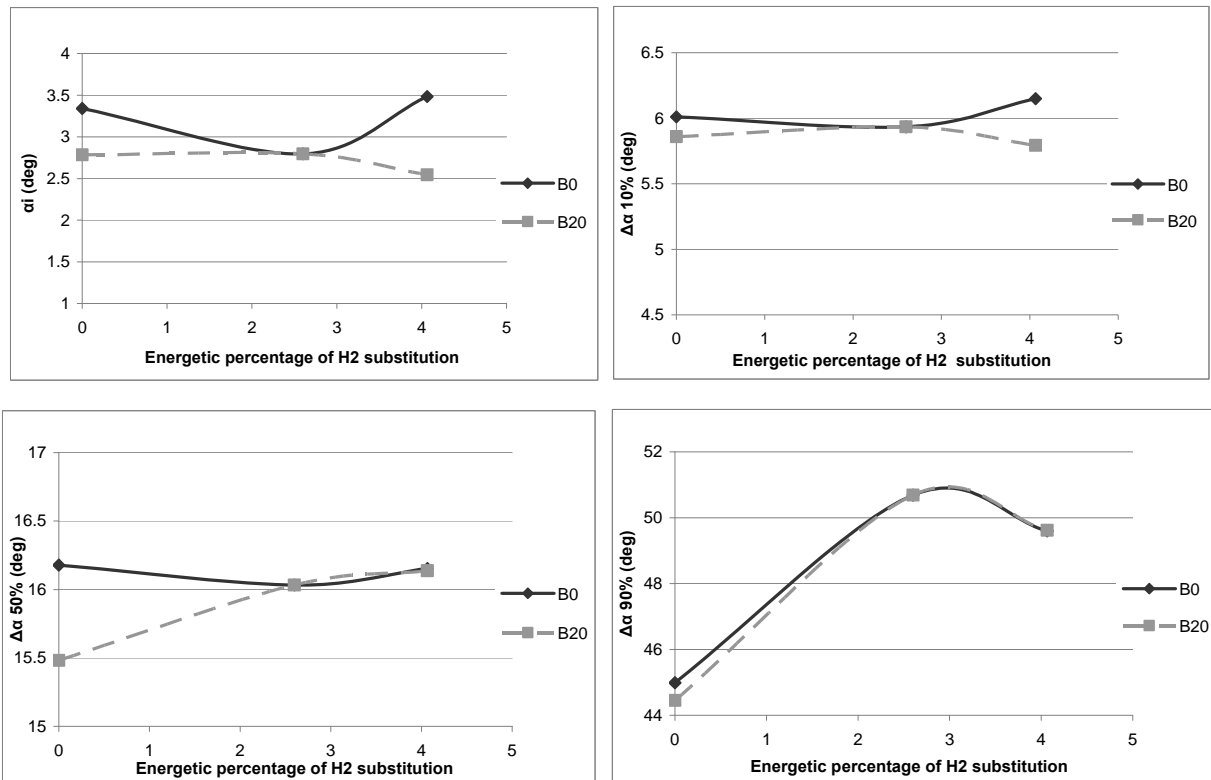


Fig. 4. Variation of the heat release characteristic moments with hydrogen percentage (energetic) at 60% load and 2400 rpm.

3.2. Emissions

Carbon Monoxide. Figure 5a shows the CO emission at 1400 rpm, which appears generally higher for B20 than for diesel fuel. The addition of 4.4% hydrogen to B20 fuel results in lower CO emission by 4%, but if the hydrogen supplement is increased to 6.9%, no additional effect is apparent. For diesel fuel, an addition of 4% hydrogen lowers CO emission by 1.6%, and with 6.9% hydrogen by 2%. A decreasing trend of CO emission with

hydrogen addition is stronger for B20 at 2400 rpm (Figure 5b): the emissions are abated by 4.5% and 10%, with 2.6% and 4.1% hydrogen, respectively. A decrease by 4% is also apparent in the case of diesel fuel, with 4.06% hydrogen.

The hydrogen addition effect on the CO emission abatement could be related to its main role in the oxidation mechanism of CO. As it is known, even small concentrations of hydrogen containing species could catalyze significantly the kinetics of CO-O₂

reaction by participation of the radical OH [20]. An explanation of the differences between the petroleum diesel fuel and B20 is less apparent.

Total unburned hydrocarbons. THC emissions are generally low and still significantly lower with B20 than with diesel fuel. Smaller THC emissions in the case of B20 could be related to the lower content in carbon compared to petroleum diesel fuel. An addition of hydrogen has not a significant additional effect (Figure 6).

Oxides of nitrogen. As shown in Figure 7, NO_x emissions are lower for B20 than for diesel fuel, and are slightly changed by hydrogen input. At 1400 rpm, an addition of 4.4% hydrogen to B20 lowers NO_x emissions by 4% and with 6.9% hydrogen only by 0.9%. At 2400 rpm, even opposite effects are found for different hydrogen concen-

trations: with a supplement of 2.6% hydrogen to B20, NO_x emission is lower by 5%, but the emission is increased by about 3% with 4% hydrogen.

In the case of diesel fuel, the enrichment with hydrogen is penalized at all hydrogen percentages: at 1400 rpm, NO_x emission is higher by 5% with 4.4% hydrogen and at 2400 rpm, higher by 2% with 2.6% hydrogen.

A specific cause of the different NO_x emissions reported for petroleum diesel fuel and B20 is not evident. The NO_x emission is currently related to the reaction temperature. For the diesel engine, the diffusion flame temperature would be the specific parameter to be considered, NO_x emission being generated mainly in the proximity of the diffusion flame. The corresponding stoichiometric adiabatic flame temperature for B20 and petroleum diesel fuel B0 are but very close, less than 1K different [12].

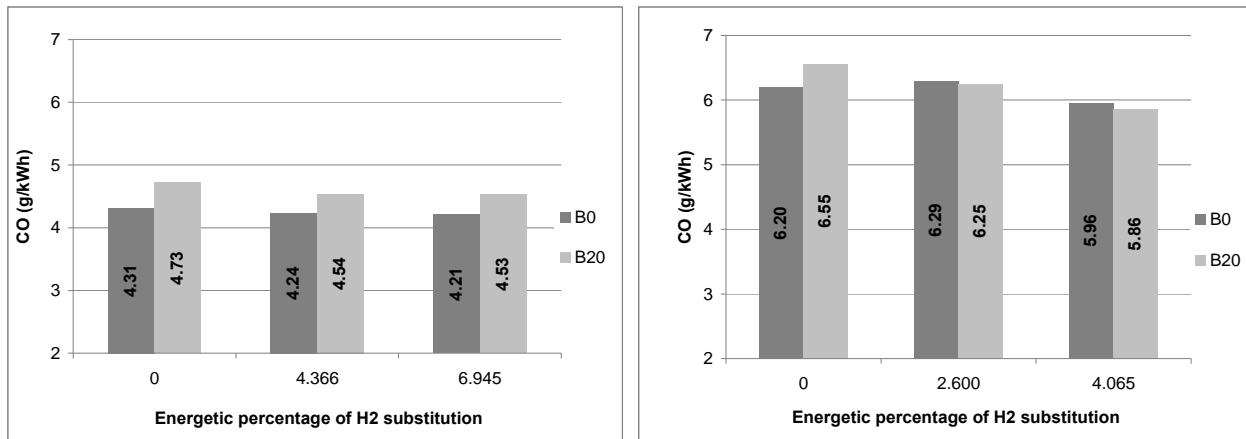


Fig. 5. Variation of CO emissions with hydrogen percentage at 60% load: a – 1400 rpm; b – 2400 rpm.

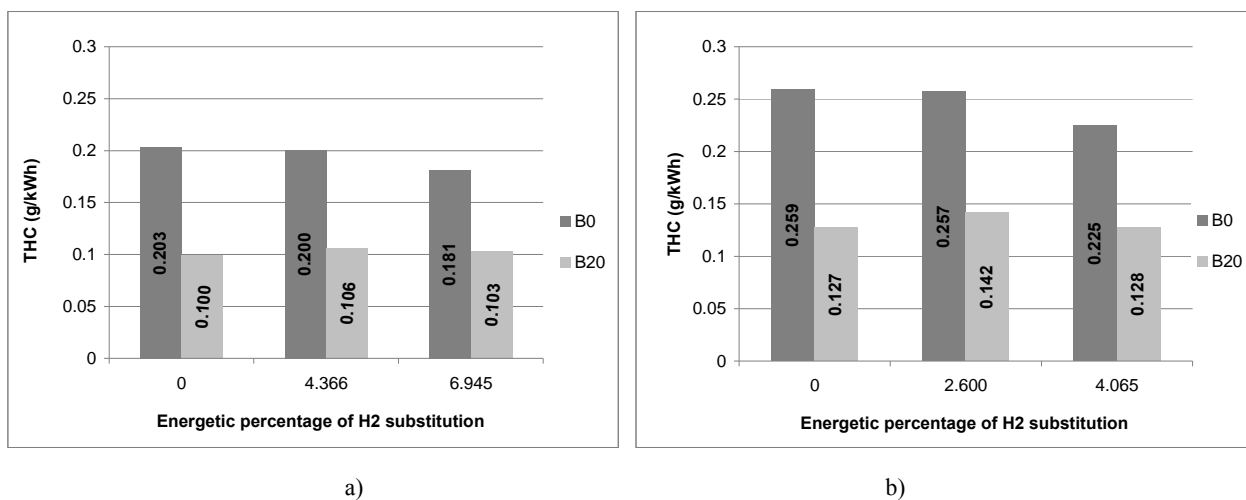


Fig. 6. Variation of THC emission with hydrogen percentage at 60% load: a – 1400 rpm; b – 2400 rpm.

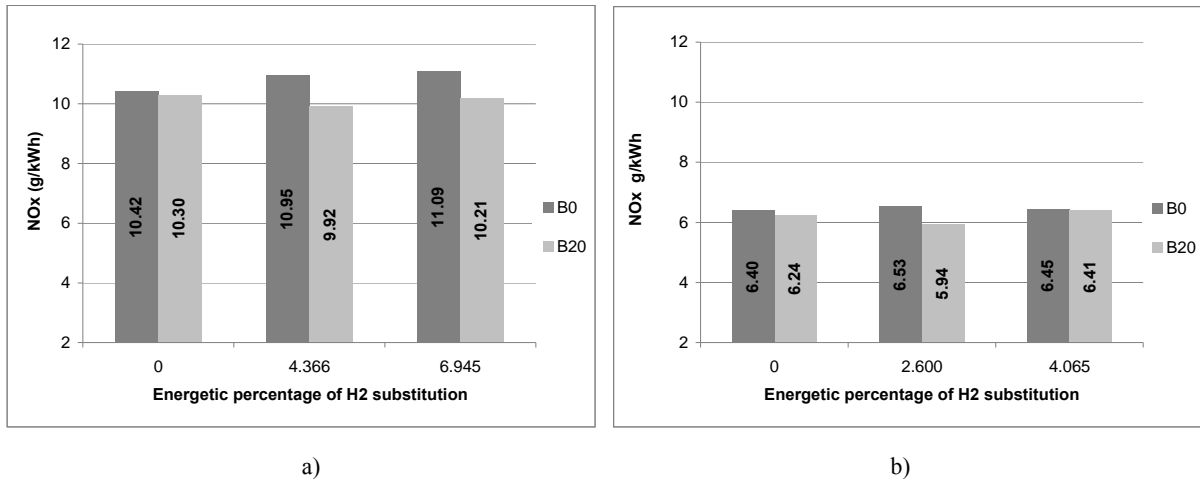


Fig. 7. Variation of NO_x emissions with hydrogen percentage at 60% load:
a – 1400 rpm; b – 2400 rpm.

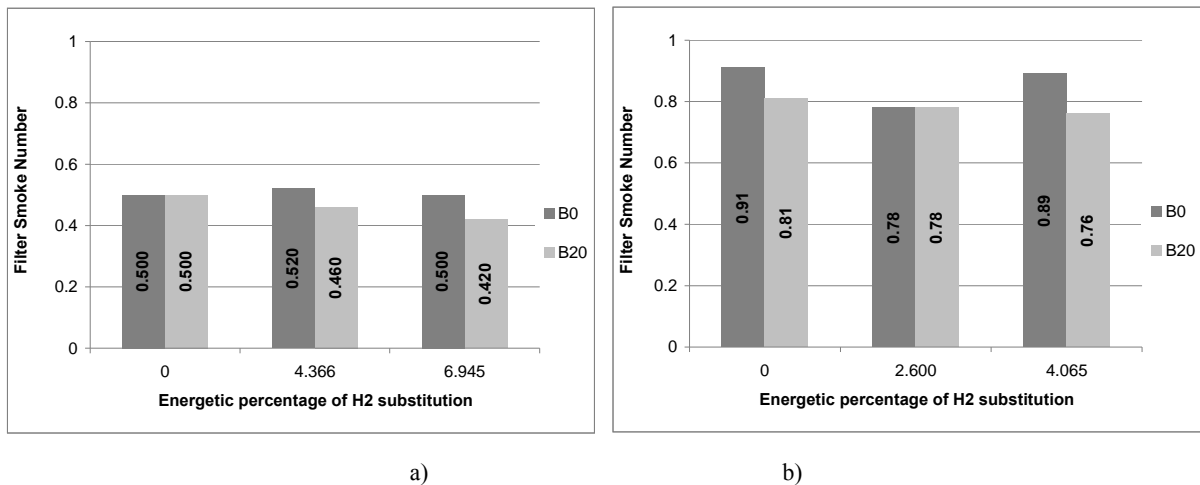


Fig. 8. Variation of the filter smoke number (FSN) with hydrogen percentage at 60% load:
a – 1400 rpm; b – 2400 rpm.

Additional influential factors could be the degree of saturation of the biodiesel — resulting in different flame temperature — and a marked temperature distribution [15]. The hydrogen addition with its specific role played in NO formation according to the “extended” Zeldovich mechanism and an eventual influence on the diffusion flame temperature could be considered in relation with the differences in NO_x emissions.

Smoke. The supplement of hydrogen to B20 fuel is beneficial in reducing smoke emission. At 1400 rpm, the filter smoke number (FSN) was decreased by 8% and 16% by the enrichment with 4.3% and 6.9% hydrogen, correspondingly (Figure 8a). At 2400 rpm, the trend was similar: a decrease by 4% and 6% with 2.6% and 4%, hydrogen correspondingly (Figure 8b).

In the case of neat diesel fuel, the smoke level is generally higher than with B20, and the influence

of hydrogen addition is not similarly coherent. At 1400 rpm, FSN was even higher by 4% with 4.3% hydrogen; at 2400 rpm, FSN was but lower by 14% and by 2% with 2.6% and 4% hydrogen, correspondingly. The reference FSN values without hydrogen are equal for B20 and diesel fuel, at 1400 rpm, and are lower by 11% for B20 at 2400 rpm.

Previous studies have generally found that biodiesel blends, eventually with the exception of B20, have lower PM emissions than petroleum diesel at full load and higher PM emissions at low load. At full load, the lower level of smoke emissions for biodiesel is currently discussed in terms of soot formation, in the fuel rich core of the jet, due to a lower concentration in aromatics and fuel-bound sulphur. The oxygen atoms introduced in this region by an oxygenated fuel like biodiesel act as soot oxidant and soot precursor suppressors, through the formation of OH radicals [15], [19]. At low

load, combustion is dominated by the premixed burn and the rate of pyrolysis and particularly the rate of oxidation attack on soot precursors are increasing with temperature [21]. Biodiesel structure could thus play a role in the sooting tendency only by an influence on the flame temperature. The present results, which were obtained at mid load operation of the engine, could thus be integrated between these two limit conditions.

The favorable effect of hydrogen addition on the filter smoke number was attributed to a change in the nature of particulate matter produced. Instead of the particulates which are ordinarily black, the hydrogen would favor the growing of more gumming and colorless particulates [19, 22, 23]. Another effect of hydrogen addition would be possible as related

to a change in temperature controlling the oxidation of the particulates.

4. RESULTS BY NUMERICAL SIMULATION

Possibilities to enhance the effects of B20 supplemental with hydrogen by changing the start-of-injection (SOI) timing were investigated by numerical simulation of the engine with AVL BOOST code v2011.1 [24]. Figure 9 shows the symbolic model of the engine with the following main elements: manifolds (1-18), plenums (PL1-PL3), junctions (J1-J5), air filter (CL1), cylinders (C1-C4), and measuring points (MP1-MP5). The boundary conditions for the intake and exhaust systems are defined by SB1-SB4.

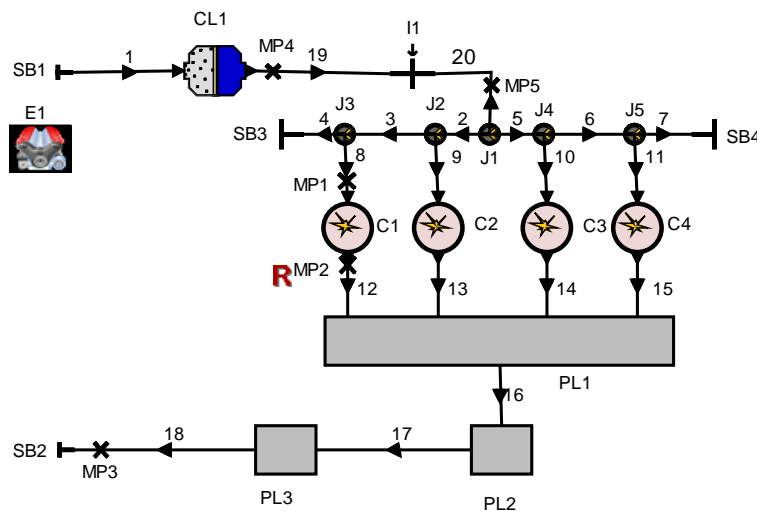


Fig. 9. Symbolic model of the engine.

The special situation for hydrogen addition by aspiration in the intake air is symbolized by the gas injector I1. The corresponding sizes and state parameters are input data. The gas flow in the intake and exhaust systems is modeled as a one-dimensional turbulent flow with pressure drops along the systems, and is defined in terms of the specific valves sizes, timings and lift characteristics, engine speed and piston kinematics. Combustion modeling is developed by the AVL -MCC model which has distinct submodels for the pre-mixed and mixing controlled phases: by a Wiebe function for the first phase and by a special one for the second phase. The related input data refer to specific parameters, combustion details like ignition delay or time interval of the premixed phase, injection process characteristics and fuel specifications. The injection process was defined in terms of the nozzle holes size, the pressure drop across the nozzle orifices, the discharge coefficient and the needle lift characteristic. The instantaneous mass flow rate through injector nozzle is expressed as functions of the

experimental needle position and the pressure difference between the upstream (line) and downstream (cylinder) pressures. Figure 10 shows the needle lift variation and the pressure variation in the high pressure line at the injector connection where the high pressure transducer is located.

Specifications of B20 were based on the neat biodiesel (soybean methyl ester) data base recently available from AVL. Modeling of NO_x emissions generation is calculated with an "extended Zeldovich" mechanism with six reactions, and is controlled by two parameters. The CO emission model implemented is based on two oxidation reactions of CO and is controlled by one parameter. The soot emission, calculated from the rate of formation and the rate of oxidation needs also two control parameters. The model was calibrated with the experimental results at 2400 rpm, for the engine fueling with neat B20 and B20 with 4% hydrogen addition. Figure 11 compares the predicted cylinder pressure and rate of heat release (ROHR) for both fueling conditions with the experimental ones.

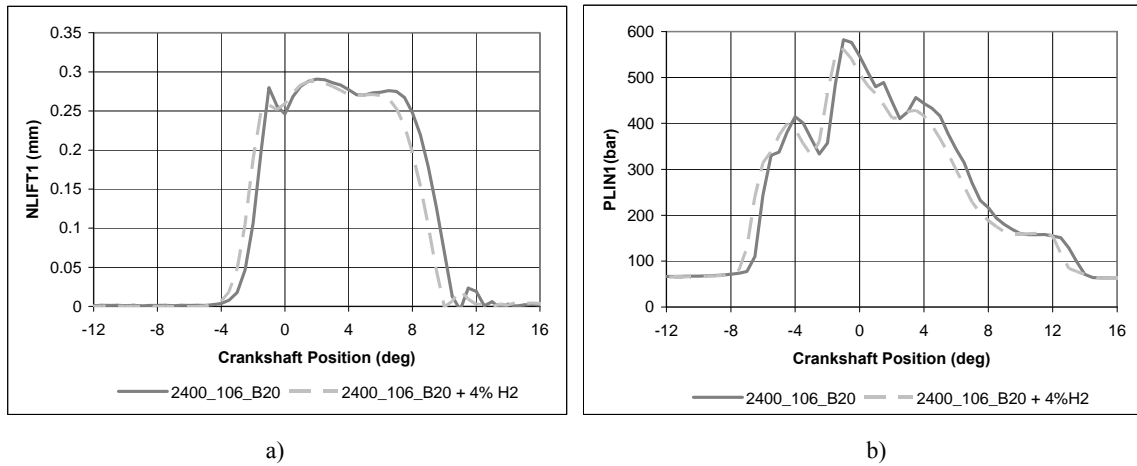


Fig. 10. Variation of injection characteristics for engine operating condition 2400 rpm and 60% load: *a* – injector needle lift; *b* – line pressure.

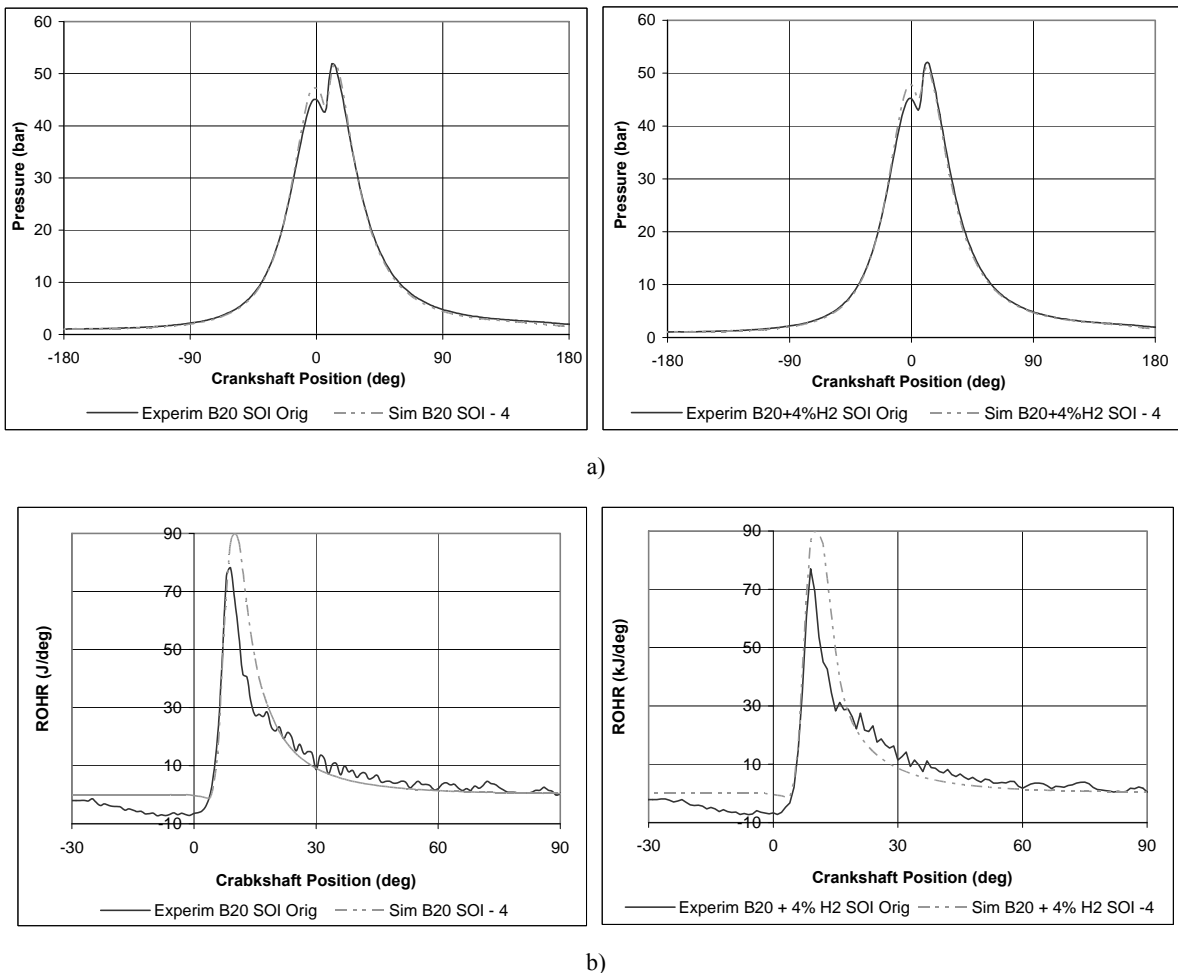


Fig. 11. Results of model calibration at 2400 rpm and -4°CA start of injection timing with neat B20 and B20 plus 4% hydrogen: *a* – cylinder pressure; *b* – rate of heat release.

The corresponding emissions are also compared in Table 2. It can be seen from these comparisons that the differences in the rates of heat release resulted in cylinder pressure errors are lower than 4.2% and emissions errors lower than 1.8% for both fueling conditions.

The simulation calculations were carried-out for neat B20 and B20 plus 4% hydrogen, with the SOI timing variable parameter advancing in the range of 0... to -20°CA . The normalized rate of injection determined for calibration stage was kept unchanged and it was shifted according to the value

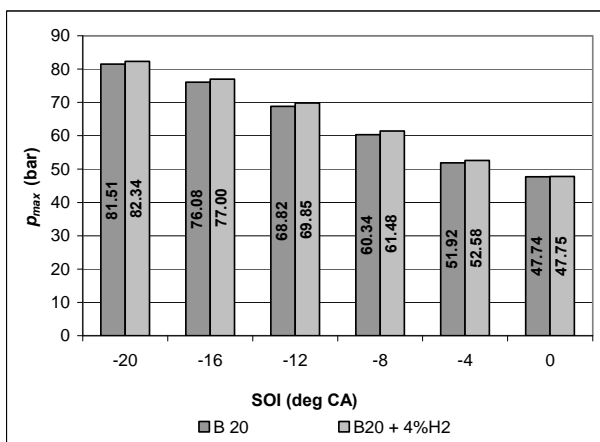
of SOI timing selected. These calculations have shown the increase of cylinder maximum pressure p_{max} by about 71% (Figure 12a) and of maximum rate of pressure rise 212%. The indicated engine efficiency increases in the same range by 7%. As was predictable, in the explored range, gradual increasing of SOI has improved performance, with the penalty of higher maximum pressure and rate of pressure rise. At any considered SOI, the effect of hydrogen addition on the indicated engine efficiency η_i is insignificant. Injection timing variations have a strong effect on CO emission (Figure 12b): the emissions of B20 are halved as the timing is advanced from -4 °CA to -20 °CA, with the

corresponding combustion temperature increase. Addition of hydrogen gives a supplemental reduction of CO emission of 5 - 6.5% in the explored range of SOI timings.

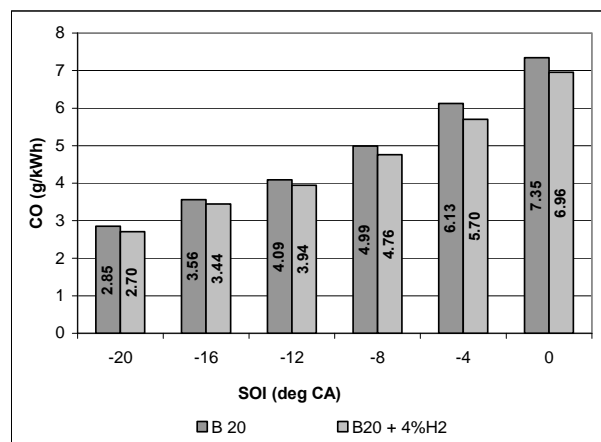
Table 2

Emissions comparison

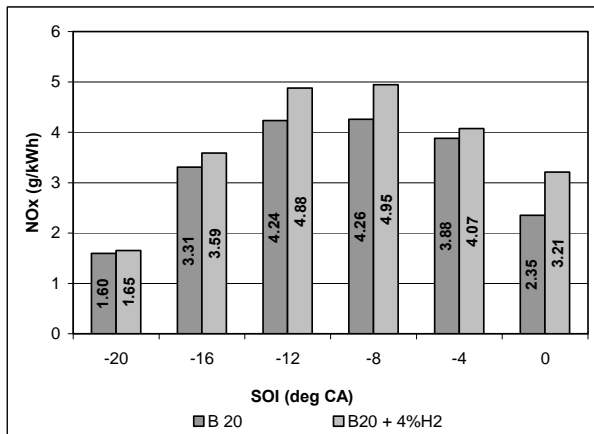
Emission		Experimental		Simulation	
		B20	B20 +4% H ₂	B20	B20 +4% H ₂
NO _x	ppm	370	394	376.6	394.6
CO	ppm	638.4	592.1	639.9	591.8
Soot	FSN	0.81	0.76	0.816	0.753



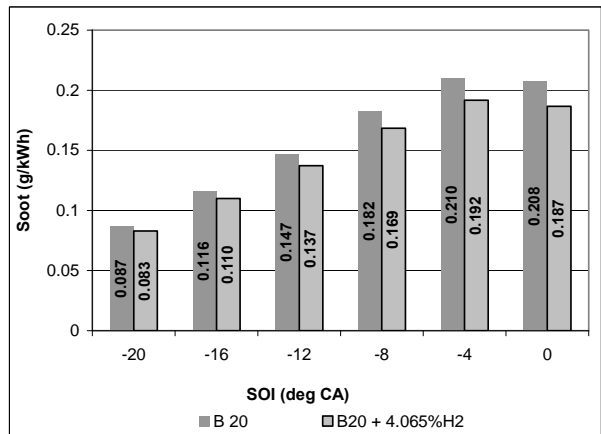
a)



b)



c)



d)

Fig. 12. Effects of SOI timings on maximum cylinder pressure and emissions at 2400 rpm and 60%load, for B20 and B20 plus 4% hydrogen: a) p_{max} ; b) CO; c) NO_x; d) Soot.

The effect of SOI timings on NO_x emissions for neat B20 and the case of B20 with 4% hydrogen are shown in Figure 12c. An increase of the emission by 10% is observed for B20, by SOI timing advance from -4 °CA to -12 °CA. A further advance to -20 °CA would but lower the emission

by 60%. The same trend is found in the case of B20 with 4% hydrogen addition and is related to the temperature effects. By SOI advancement higher temperatures are achieved markedly in the diffusion flame and also post-flame, promoting the NO formation. A specific cause for the NO_x emission

decrease beyond the advance of SOI timing of 12 °CA was not identified.

Figure 12d shows the effect of SOI timings on soot emission from B20 and B20 with 4% hydrogen. The emission is rapidly decreasing with the advancement of B20 injection timing and at -20 °CA advance the emission is 2.3 times lower than at -4 °CA.

The resemblance between the effects of SOI timing variations on CO and soot for neat B20 or with 4% added hydrogen is apparent and emphasizes the similarity of the temperature influence on the oxidation process, with the radical OH playing a leading role in both cases.

5. CONCLUSIONS

Effects of a 20% biodiesel blend (B20) were studied experimentally and by engine simulation on a tractor diesel engine operating at 60% load and 1400 rpm, or 2400 rpm. The major conclusions are the following:

- BTE and the heat release characteristic of B20 are practically not different from petroleum diesel fuel. Different emissions were but detectable. At 1400 rpm, B20 had higher CO emissions by 9% relative to petroleum diesel and lower emissions of unburned hydrocarbons (THC) by 50%; NO_x and smoke emissions were almost equal. At 2400 rpm, CO emissions were higher by 6% and THC, NO_x, and smoke emissions lower by 50%, 2.5% and 11% respectively compared to petroleum diesel fuel.

- A supplement of hydrogen by aspiration in the intake air flow has generally insignificant effects on BTE and heat release characteristic, except the duration of the last part of the mixing-controlled combustion phase, which is delayed. With 7% hydrogen at 1400 rpm, the smoke emission of B20 was reduced by 16%; reductions by 6% and 1% were also found for CO and NO_x emissions. With 4% hydrogen at 2400 rpm, the smoke emission of B20 was abated by 6% and CO emission by 10%, while NO_x was increased by 3%. Petroleum diesel fuel was less sensitive to hydrogen supplements.

- Engine performance and emissions can be strongly improved by relatively small alterations of the start-of-injection (SOI) timings, with the predictable shortcomings of higher maximum in-cylinder pressure and rate of pressure rise. For B20, with 4% hydrogen and at 2400 rpm, the advancement of SOI timing from -4 °CA to -8 °CA, lessened soot emissions by 12% and CO emission by 22% with a penalty of NO_x emission increase by 21%. Effects of B20 can thus be significantly

improved with a small amount of hydrogen and the advancement of SOI timing corresponding to a rational trade-off between emissions and in-cylinder pressure effects.

Acknowledgements

The authors of this paper acknowledge the AVL Advanced Simulation Technologies team for its significant support offered to them in performing the simulation part of this work.

REFERENCES

- [1] Geyer MS, Jacobus MJ, Lestz SS. *Comparison of diesel engine and performance and emissions from neat and transesterified vegetable oils*. Trans. of the ASAE; 1984, 27, 375-381.
- [2] Alfuso M, Auriemma M, Police G, Prati MV. *The effect of methyl ester of rapeseed oil on combustion and emissions of a DI diesel engine*. SAE Paper; 1993 [932801].
- [3] Last RJ, Kruger M, Dumholz M. *Emissions and performance characteristics of a 4 stroke DI diesel engine fueled with blends of biodiesel and low sulfur diesel*. SAE Paper; 1995 [950054].
- [4] Graboski MS, Ross JD, McCormick RL. *Transient emissions from No2 diesel and biodiesel blends in a DDC series 60 engine*. SAE Paper; 1996 [961166].
- [5] Schmidt K, van Gerpen JH. *The effect of biodiesel fuel composition on a diesel combustion and emissions*. SAE Paper; 1996 [961086].
- [6] Hansen KF, Grouleff JM. *Chemical and biological characteristics of exhaust emissions from a DI diesel engine fueled with biodiesel and diesel fuel*. SAE Paper; 2000 [2000-01-1967].
- [7] Senatore A, Cardone M, Rocco V, Prati MV. *A comparative analysis of combustion process in D.I. diesel engine fueled with biodiesel and diesel fuel*. SAE Paper; 2000 [2000-01-0691].
- [8] Sharp, CA, Howell SA, Jobe J. *The Effect of Biodiesel Fuels on Transient Emissions from Modern Diesel Engines, Part I Regulated Emissions and Performance*, SAE Paper; 2000 [2000-01-1967].
- [9] Monyem A, van Gerpen JH. *The effect of biodiesel oxidation on engine performance and emissions*. Biomass and Bioenergy 2001;20:317-325.
- [10] Bielaczyc P, Szczotka A, Gizynski P, Bedyk I. *The effect of pure RME and Biodiesel Blends with High RME Content on Exhaust Emissions from a Light Duty Diesel Engine*. SAE Paper; 2009 [2009-01-2653].
- [11] Ma F, Hanna MA. *Biodiesel production: a review*. Bioresource Technology 1999;70:1-15.
- [12] Sun J, Caton JA, Jacobs TJ. *Oxides of nitrogen emissions from a biodiesel fuelled diesel engines*. Progress in Energy and Combustion Science 2010;36:677-695.
- [13] Agarwal AK. *Biofuels (alcohols and biodiesel) applications as fuels for internal combustion engines*. Progress in Energy and Combustion Science 2007;33:233-271.
- [14] Lapuerta M, Armas O, Rodríguez-Fernández J. *Effect of biodiesel fuels on diesel engine emissions*. Progress in Energy and Combustion Science 2008;34:198-223.
- [15] Choi CY, Reitz RD. *An experimental study on the effects of oxygenated fuel blends and multiple injection strategies on DI diesel engines emissions*. Fuel 1999; 78:1303 – 1317.

- [16] Lilik GK, Zhang H, Herreros JM, Haworth UC. *Hydrogen assisted diesel combustion*. Int. J Hydrogen Energ 2010;35:1-17.
- [17] Liew C, Li H, Liu S, Besch MC, Ralston B, Clark N. *Exhaust emission of a H₂- enriched heavy-duty diesel engine equipped with cooled EGR and variable geometry turbocharger*. Proc. ASME 2010 Internal Combustion Engine Division Fall Technical Conference, San Antonio, Texas, USA; 2010.
- [18] Birtas A, Voicu I, Petcu C, Chiriac R, Apostolescu N. *The effect of HRG gas addition on diesel engine combustion characteristics and exhaust emissions*. Int. J Hydrogen Energ 2011;36:12007-12014.
- [19] Bika AS, Franklin ML, Kittleson D. *Emissions effects of hydrogen as a supplemental fuel with diesel and biodiesel*, SAE Paper; 2008 [2008 – 01 – 0648].
- [20] Glassman I. *Combustion*, Second ed. New York Academic Press; 1987.
- [21] Frenklach M, *Kinetics and mechanism of soot formation on hydrocarbon combustion*. Final Technical Report to NASA – Lewis Research Center; 1985, Pennsylvania State University; 1990.
- [22] McWilliam L. *Combined hydrogen combustion: an experimental investigation into effects of hydrogen addition on exhaust gas emissions, particulate matter size distribution and chemical composition*. PhD Thesis, Brunel University, U.K.; 2008.
- [23] Voicu I. *Contribution to the study of biodiesel combustion in compression ignition engine* (in romanian), PhD Thesis, University Politehnica of Bucharest, Romania; 2011.
- [24] AVL BOOST. Users Guide v2011.1; 2011.